

Experimental Dynamics of Wing Assisted Running for a Bipedal Ornithopter

Kevin Peterson and Ronald S. Fearing

Abstract—BOLT is a lightweight bipedal ornithopter capable of high-speed dynamic running and effecting transitions between aerial and terrestrial locomotion modes. The gait dynamics of both quasi-static and dynamic locomotion are examined through the use of an on-board accelerometer, part of a one gram electronics package also containing a processor and radio. We discuss the accelerations in the context of the traditional spring-loaded inverted pendulum model seen in nearly all legged locomotion in organisms. Flapping wings are shown to provide damping along with propulsive force. The aerodynamic forces of the flapping wings also impart passive stability to the robot, enabling it to run bipedally with only a single actuator. BOLT transitions from ground running to aerial hovering in as little as one meter of runway. Overall, the advantages provided by wings in terrestrial locomotion, coupled with aerial capabilities, allow BOLT to navigate complex three dimensional environments, switching between locomotion modes when necessary.

I. INTRODUCTION

Navigating complex three dimensional environments is an ability that is seemingly trivial for small animals, yet provides significant challenges for robots today. Small, mobile robots (mass on the order of grams, linear dimensions on the order of centimeters) provide many advantages when exploring an environment, and are capable of operating in small spaces unreachable by a larger robot. In addition, their small size allows multiple robots to be transported and deployed, greatly increasing the amount of area they can cover.

While there are many advantages to small robots, there are also many obstacles they have trouble navigating. Obstacles much larger than the robot present a significant challenge in legged locomotion, and even robots with the ability to climb up obstacles would be impeded when confronted with an aquatic obstacle. In confined spaces, aerial robots are often unable to navigate, giving an advantage to a terrestrial robot. Flying also requires a large amount of energy, and no robot can stay aloft indefinitely. Terrestrial locomotion may be more energy efficient for shorter distances, and would allow for locomotion even if the energy for flight is spent. By being capable of both aerial and terrestrial locomotion,

This work was supported by the United States Army Research Laboratory under the Micro Autonomous Science and Technology Collaborative Technology Alliance

Kevin Peterson is with Department of Electrical Engineering and Computer Sciences, University of California, Berkeley, CA 94720, USA kevincp@eecs.berkeley.edu

Ronald S. Fearing is with Department of Electrical Engineering and Computer Sciences, University of California, Berkeley, CA 94720, USA ronf@eecs.berkeley.edu

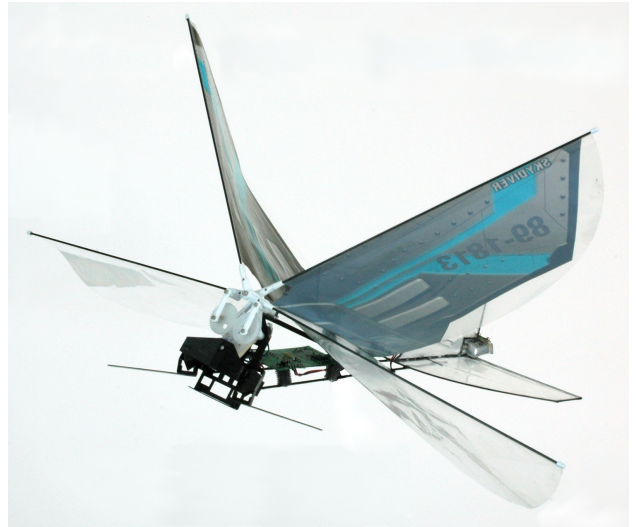


Fig. 1. BOLT: a bipedal ornithopter capable of both aerial and terrestrial locomotion.

a hybrid robot could choose the best mode of locomotion given the obstacles confronting it.

Many successful small terrestrial robots have been previously developed, including DASH [1], DynaRoACH [2], Mini-Whegs [3], Sprawlita [4], iSprawl [5], and RHex [6]. With the exception of Mini-Whegs, these robots all use six legs arranged in an alternating tripod configuration for passive stability when running. In contrast, dynamic bipedal running has generally required a complex controller and multiple actuators to maintain stability. Dynamic bipedal running has been previously demonstrated by RHex [7], along with an extensive list of larger bipedal robots. At the very small scale, dynamic bipedal running can be seen in the cockroach *Periplaneta americana* when it is running at its fastest speeds [8]. The locomotion dynamics of these robots is characterized by the spring loaded inverted pendulum model (SLIP) [9], a pattern exhibited by nearly all legged organisms despite widely varying leg numbers [10].

There have also been many ornithopters capable of hovering in an indoor environment, namely DelFly II [11], a hummingbird sized ornithopter developed by Nathan Christner [12], and the Aerovironment Nano Hummingbird [13]. Previous work on small hybrid robots includes MALV [14] and its descendant MMALV [15], the SkyhopperTM by WowWeeTM, and the EPFL microglider [16] currently under development. Work has also been done on aerial-terrestrial transitions, with [17] and [18] both capable of wall perching.

Other hybrid robots which have been developed primarily focus on terrestrial and aquatic locomotion such as Boxybot [19] and AQUA, a waterproof version of RHex [20].

The Bipedal Ornithopter for Locomotion Transitioning, or BOLT (Fig. 1), is a small lightweight robot capable of both aerial and terrestrial locomotion modes. The integration of an electronics package allows two-way communication and the investigation of the robot dynamics with a six-axis inertial measurement unit (IMU). BOLT has a total weight of 11.4 grams, with a wingspan of 28 cm and a length of 17.5 cm. The robot is capable of dynamic high-speed bipedal locomotion by exploiting its aerodynamic properties for stability. The use of aerodynamics during bipedal locomotion has been previously seen in some birds [21], although generally only in inclined running. BOLT can transition from terrestrial locomotion to hovering in as little as one meter of space, and has demonstrated the ability to takeoff on smooth tile, foam, carpeted flooring, and plywood. BOLT can also take off from inclined ledges, with up to a 45 degree slope tested. The Smart Composite Microstructures (SCM) [22] process allows the integration of a lightweight leg structure with the rest of the body, comprised mainly of carbon fiber spars.

II. MECHANICAL DESIGN

The primary design goal for BOLT is developing a platform capable of both terrestrial and aerial locomotion. To accomplish this goal, we combine the gearbox and wings from a commercial ornithopter (Air Hogs™ V-wing Avenger™) with a custom airframe, leg design, and electronics package. Because of the desire for stable hovering flight, weight and weight distribution are a key consideration in all design decisions. A single motor drives both the leg and the wings, allowing sufficiently high power density to maintain hovering flight.

A. Airframe Design

BOLT's airframe uses carbon fiber spars for structural rigidity. The lightweight properties of carbon fiber make it ideal for use in a flying platform. A rigid airframe is critical in preventing serial compliance from reducing the wing thrust. To create a lightweight tail, carbon fiber spars are placed in a cardboard pattern and a 12.7 μm film of polyethylene terephthalate (PET) is overlaid and attached to the spars with cyanoacrylate (Fig. 2(a)). The construction materials of the tail are similar to those used in [11], a successful ornithopter on the same size scale as BOLT.

The center of mass location of the robot is important for determining the posture of the robot when it is in the air. We place the battery at the very posterior of the robot on the tail, while the controller board is placed within the airframe. This gives the robot a vertical posture, with the majority of the wing thrust directed downward. By adjusting the position of the controller board, the robot can be set to either hover in place or fly forward at a slow rate. The airframe of the robot also protects the controller board during operation.

Directly mounting the controller board to the rigid carbon fiber airframe overwhelms the accelerometer due to the high

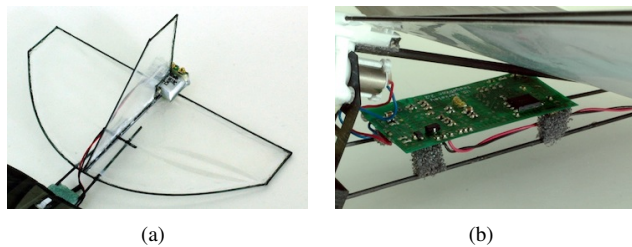


Fig. 2. (a) shows the tail of the robot, constructed from carbon fiber spars and 12.7 micron thick PET film. The battery is placed at the back of the tail to maintain proper weight distribution. (b) shows the controller board mounted on small foam offsets. The foam offsets are critical for dampening the high frequency vibrations of the body.

frequency vibrations produced by the motor transmission. To accurately study the dynamics of the robot, the board is moved forward and placed on foam mounts (Fig. 2(b)) to dampen the vibration noise and improve the quality of the acceleration measurements.

A critical feature enabling ground-to-air transitions of the robot is the angle of attack of the wings. The clap-and-peel design of the wings produces force directed perpendicularly to the stroke plane. On the initial iterations of BOLT, the wings had a low angle of attack, directing propulsive force horizontally when running along the ground. This robot was capable of flight, but could only takeoff by running from a one meter or higher ledge. Once in the air, the center of mass location caused the tail to swing under the robot and it entered a stable flight posture. Increasing the wing angle of attack allows the robot to build lift as the forward speed increases, eventually causing the robot to pitch upwards, directing the main flapping force downwards. This leads to takeoff from the ground and the robot entering a stable flight posture due to the center of mass location with respect to the center of lift. On BOLT, the angle of attack is set to 28 degrees. This value was chosen experimentally to provide a balance between the robot's maximum terrestrial speed, and the distance required for takeoff.

B. Leg Design

BOLT has a bipedal leg design, with each leg going through a symmetrical motion 180 degrees out of phase with the another. The legs are built using the SCM process [22], which allows the implementation of a lightweight structure that transforms the output of the motor to the desired leg trajectory. Four layers of unidirectional carbon fiber prepreg are sandwiched around 50.8 μm PET to create the leg structure. The layers of the unidirectional carbon fiber are arranged crosswise to provide stiffness in two directions, and are mirrored across the flexure layer. The structure is designed to provide protection to the hips in case of high velocity impacts, while allowing the legs to still extend in front and below the body.

Fig. 3 shows a simplified version of the mechanisms that transform the rotation of the motor in the transverse plane of the robot to the desired leg trajectories. A set of parallel four-bars drives the vertical motion of the legs (Fig. 3(a)),

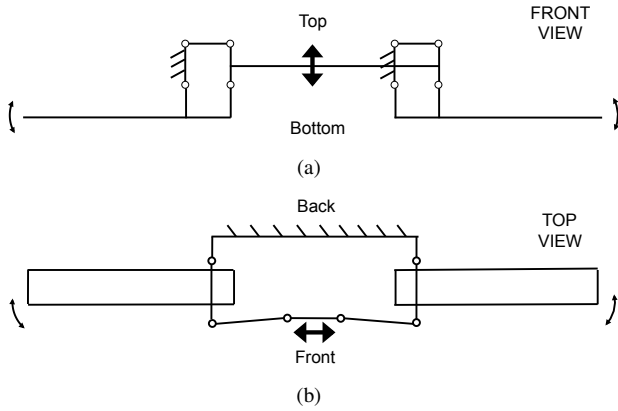


Fig. 3. Simplified representation of the mechanisms that enable the (a) vertical motion and (b) fore-aft motion of the legs.

TABLE I
PHYSICAL PARAMETERS AND COMPONENTS OF BOLT

| | |
|------------------|-----------------------------------|
| Total Mass | 11.4 grams |
| Body Size | 17.5 x 28 x 15 cm |
| Battery | Full River 60 mAh lithium polymer |
| Micro-controller | Microchip dsPIC33F |
| Communications | Atmel AT86RF231 |
| Accelerometer | Analog Devices ADXL345 |
| Gyroscope | Invensense ITG-3200 |

while a crank-slider mechanism drives the fore-aft motion of the legs (Fig. 3(b)). One revolution of the motor output gear (hereafter referred to as a single motor cycle) corresponds to a full left and right leg stride, and a single complete wing beat (opening stroke and closing stroke). In implementing the mechanisms shown in Fig. 3, several implementation details are necessary due to the properties of the SCM process. The structure is designed such that each of the flexures is in a straight default configuration, reducing the effect of off-axis forces and minimizing the strain of the PET (Fig. 4(a)). The motion of the legs is shown in Fig. 4, and in the companion video.

C. Power, Communications, and Control

BOLT uses a custom electronics package (ImageProc 2.2) that incorporates a 40 MHz dsPIC processor with a motor driver, six-axis IMU, and 1 MB of Flash memory (Table I) [23]. In addition, the board has an Atmel 802.15.4 radio for communication with a laptop. A Python interface sends commands to the robot and receives data from the board's sensors. A 60 mAh battery powers the electronics board and motor.

III. METHODS AND RESULTS

BOLT has two regimes of operation when locomoting terrestrially, a quasi-static gait (9 Hz) and a dynamic gait (12.5 Hz). To study the dynamics in each of these modes, we use the accelerometer to examine the intra-stride forces at steady-state velocity. The rate gyroscope allows the acceleration data to be corrected for the pitch and roll of the body,

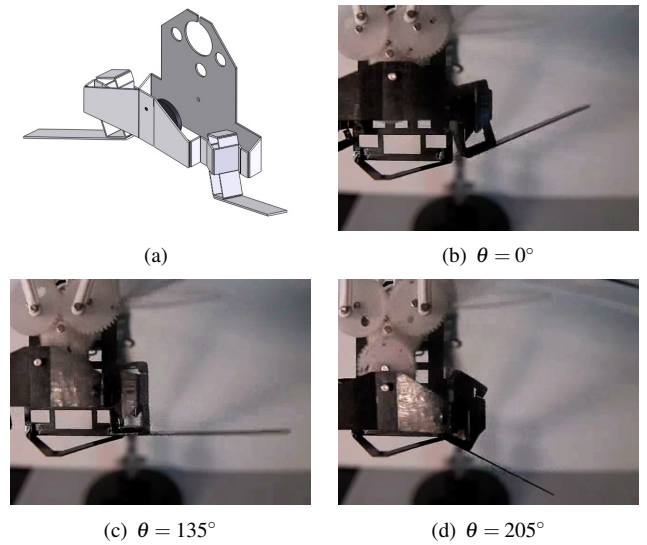


Fig. 4. The implementation of the mechanism described in Fig. 3 is shown by (a). Here, the movable flexures have been straightened, reducing the strain and the effect of off-axis forces. (b)-(d) show screenshots from the companion video of the left leg moving through its stride. The right leg exhibits similar motion in anti-phase with the left.

aligning the acceleration components in the horizontal and vertical directions. We use the maximum velocity obtained by the robot as a relative measure of the maximum effective locomotive force on the robot. The data are parameterized by the output gear phase, obtained by integrating the highly periodic back EMF signal. By performing the tests on carpet, we ensure the legs have good traction with the ground during the trials.

We consider two control cases to distinguish between the force contributions of the flapping wings and the legs when running along the ground. We replace the legs on BOLT with lightweight wheels (Fig. 5(a)) to isolate the effects of the flapping wings (wings-only, WO). In this configuration, the flapping wings supply all of the locomotive force. Removing the linkage driving the wings (Fig. 5(b)) reduces the wings to a passive element with the locomotive force coming entirely from the legs, (wings-passive, WP). This configuration also allows the differentiation between the effects of flapping the wings and the passive properties of the airfoil.

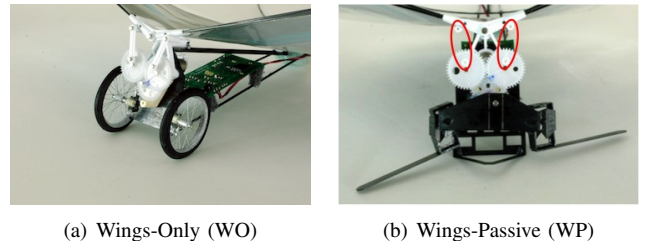


Fig. 5. (a) shows the first control case, the robot with wheels instead of legs, allowing the investigation of the wing effects alone. For the second control case (b), we disconnect the linkage driving the wings, removing any active effects from flapping.

TABLE II

FORWARD VELOCITY (m/s), MOTOR INPUT POWER (W), AND COST OF TRANSPORT ($J/(kg \cdot m)$) FOR DIFFERENT CONFIGURATIONS AND GAITS

| Gait (frequency) | | Configuration | | |
|------------------------|----------|---------------|------------|--------|
| | | Wings-Passive | Wings-Only | Hybrid |
| Quasi-static (9 Hz) | Velocity | 0.33 | 0.17 | 0.50 |
| | Power | 0.36 | 0.65 | 0.89 |
| | COT | 96.8 | 337.4 | 155.8 |
| Dynamic (12.5 Hz) | Velocity | 0.35 | 1.5 | 1.5 |
| | Power | 0.36 | 0.79 | 0.91 |
| | COT | 89.7 | 45.9 | 53.1 |

A. Quasi-static Terrestrial Locomotion

BOLT exhibits a quasi-static walking gait when running at a flapping frequency of 9 Hz. The aerodynamic effects of the flapping wings are minimal in this gait, with the WO robot reaching a maximum velocity of 0.17 m/s. In contrast, the legs of the WP robot propel it at 0.33 m/s. Overall, the hybrid robot reaches 0.5 m/s, suggesting a superposition of the leg and wing thrust components may explain the hybrid gait.

Fig. 6 shows the fore-aft and vertical accelerations of the robot over a representative cycle. We show the accelerations for the WO robot, the WP robot, the superposition of the WO and WP robots, and the hybrid robot. The accelerations of the hybrid robot are similar in both magnitude and shape to the superposition of the WO and WP robots, suggesting a lower degree of interaction between the leg and wing forces in this gait. An effect of leg/wing force coupling that can be seen is the smoother accelerations of the hybrid robot compared to those the WO+WP model predicts. The flapping wings provide a higher amount of dampening on the impulsive leg forces the robot generates than the passive wings.

The motor velocity over a representative cycle of the quasi-static gait is shown in Fig. 7. The robot uses constant PWM control for the motor, causing the motor velocity to vary dependent upon load. Over a single cycle, the effect of the varying load due to the flapping wings or legs is seen clearly from the change in motor velocity. The variation in motor velocity for the hybrid robot and the WO robot is nearly identical, implying a similar load in the two cases. Thus, despite the wings ineffectiveness in this gait they are responsible for the majority of the power consumption of the motor. Table II shows the WO robot consumes 80% more power than the WP robot despite traveling at only half the speed. This is reflected by the cost of transport: the WP robot is the most efficient while the WO robot is the least efficient. The hybrid robot has an efficiency between the two controls.

B. Dynamic Locomotion

The second running gait of BOLT is dynamic bipedal locomotion, seen at a flapping frequency of 12.5 Hz. The aerodynamic force the flapping wings provide increases greatly, with the WO robot running at 1.5 m/s. The hybrid robot also runs at 1.5 m/s, while the WP robot is only capable

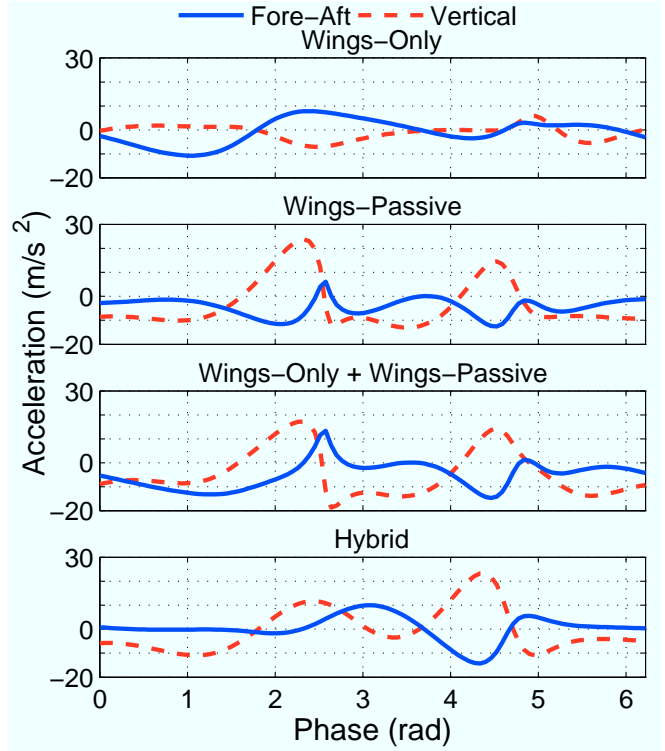


Fig. 6. Fore-aft and vertical accelerations shown over a single representative cycle when running at 9 Hz at a steady state velocity. At slow frequencies the robot exhibits quasi-static motion. In this regime, the forces on the hybrid robot are consistent with the superposition model of the individual leg and wing forces.

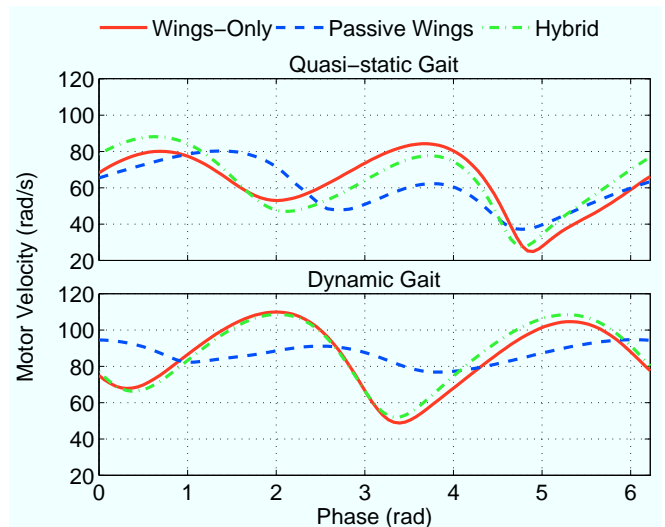


Fig. 7. Motor velocity over a representative cycle for both the quasi-static gait (9 Hz) and the dynamic gait (12.5 Hz).

of 0.35 m/s. In this gait, there is a strong interaction between the wing and leg dynamics.

The acceleration plots of Fig. 8 show the same four cases as above (WO, WP, WO+WP, Hybrid), along with a fifth case: the WO case subtracted from the hybrid case. For this gait, the WO+WP model is a poor predictor of the hybrid accelerations, predicting magnitudes over double the measured values.

The WP case shows one overly large single acceleration caused by a footfall centered at a phase of π , propelling the robot into the air preventing the next footfall from generating the same amount of force. Between footfalls, the robot is in free-fall, with zero fore-aft acceleration, and a vertical acceleration of $-9.8m/s^2$. The high accelerations and gait asymmetry of the WP case are generally indicative of poor leg tuning on a robot with a traditional SLIP gait. The hybrid robot uses the same legs as the WP robot at the same frequency, but the accelerations experienced by the robot are much lower. We again see the effect of the flapping wings dampening the leg impulses from the quasi-static case, but to a higher degree now. The hybrid robot does not have the free-fall state shown by the WP robot; stopping this free-fall leads to the high accelerations seen in the WP case. The hybrid robot is “flying between footfalls” instead of falling, greatly reducing the accelerations that must be effected by the legs.

The WO robot and the hybrid robot both run at the same forward velocity and motor frequency (see Fig. 7). This leads to the assumption that the wing forces are nearly the same in both cases regardless of the ground contacts. Subtracting the WO case from the hybrid case shows the leg forces for the hybrid robot. While they still differ from a traditional SLIP gait due to the leg/wing interactions, the legs no longer appear poorly tuned. From this data, we conclude a flapping wing robot should use stiffer legs than would normally be expected for a robot running with legs alone.

The motor velocities, and thus the dynamic loading, are nearly identical between the hybrid robot and the WO robot during the dynamic gait (Fig. 7). As in the quasi-static case, the WP robot uses the least amount of power, followed by the WO robot with the hybrid robot consuming the most power (see Table II). Due to the differing forward speeds the COT relationship is now markedly different, with the WO case the most efficient and the WP case the least efficient. Once again, the hybrid provides a compromise between the cases.

C. Terrestrial to Aerial Transitions

By running along the ground at a high speed, BOLT can generate enough aerodynamic lift to take off. Depending upon the center of mass location, BOLT requires between one and two meters of runway space. Fig. 9 shows the robot during a takeoff maneuver with the controller board mounted forward, causing a takeoff distance just under 2 meters when flapping at 18 Hz. The average acceleration for each stride is shown, along with the instantaneous velocity obtained by integrating the accelerometer data. BOLT accelerates very quickly from a standstill, reaching 1 m/s in 0.14 s and 2

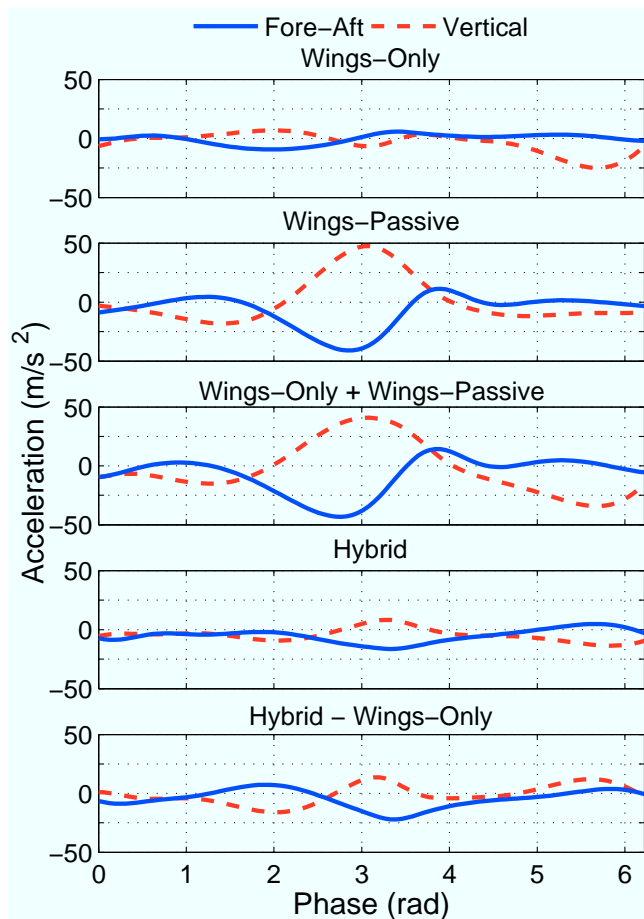


Fig. 8. Fore-aft and vertical accelerations shown over a single representative cycle when running at 12.5 Hz. At high speeds, a simple superposition of the leg and wing forces does not accurately predict the overall force on BOLT. The interactions between the legs and the wings are an important component of the forces during dynamic locomotion, altering the range of leg stiffnesses that give stable locomotion.

m/s in 0.38 s. Upon reaching a velocity of 2.5 m/s, BOLT has taken off and is no longer touching the ground. The robot continues to accelerate until reaching 3 m/s. At this point the tail begins to swing under the robot and it enters a vertical flight posture. The vertical accelerations oscillate around zero throughout the maneuver as the robot bounces along the runway. The total vertical velocity stays very near zero however, as the accelerometer does not pick up the slow movement upwards of the robot.

By moving the location of the controller board (and the center of mass), BOLT can be configured to have different transition properties. Moving the controller board forward increases the distance required for takeoff (~ 2 m), but also increases the maximum terrestrial speed (2.5 m/s). Additionally, it allows the board to be placed on foam offsets, improving the IMU measurements. When the board is moved to the back of the airframe, the takeoff distance is reduced to 1 meter. The speed where takeoff occurs is also reduced to 1.75 m/s.

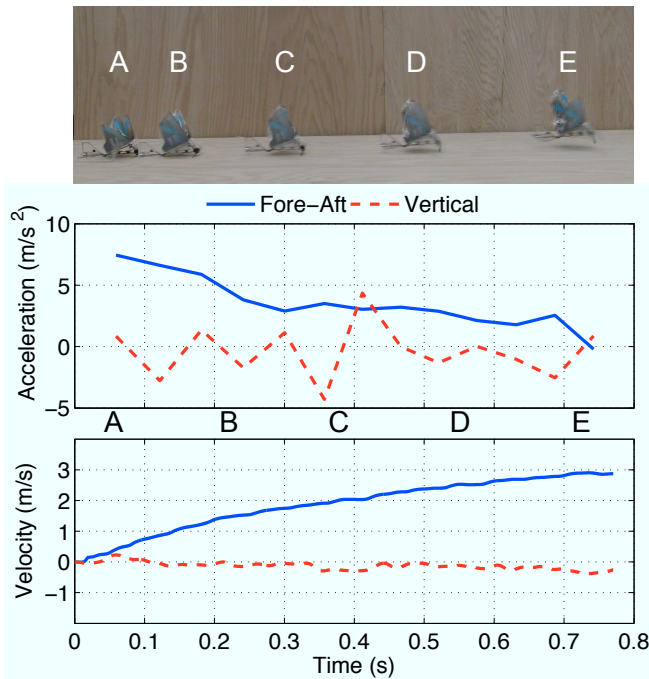


Fig. 9. BOLT transitioning from terrestrial locomotion to aerial locomotion. The average acceleration of each stride/wingbeat is plotted, along with the velocity obtained by integrating the accelerometer data. The robot quickly builds speed (A-C), lifting off at 2.5 m/s (D) and continuing to accelerate until it reaches 3 m/s (E). The vertical acceleration oscillates around zero, giving near zero vertical velocity throughout the run.

IV. DISCUSSION

The method BOLT uses to maintain stability when running differ between the quasi-static and dynamic gait. At low speeds, the tail of the robot remains in contact with the ground and provides an extra point of stability. At higher speeds, the tail of the robot lifts off of the ground, and the robot is truly bipedal. The aerodynamic forces from the flapping wings and the tail allow the robot to maintain passive stability despite its bipedal locomotion in the absence of any closed loop control. The sprawled posture of the legs and low-to-the-ground design help the robot maintain stability during both modes of locomotion.

By using the flapping wings to provide additional thrust, the terrestrial speed of the robot is significantly increased from a legged robot. With a quasi-static gait, the wings-passive robot has the best COT, while the wings-only robot performed best at a dynamic gait. The hybrid robot provides a compromise between the two, allowing more efficient locomotion when a range of speeds is necessary. At slow speeds legs provide more efficient thrust than wing flapping; at high speeds the wings allow the robot to “fly” along the ground, dramatically reducing the cost of transport.

BOLT has also shown the ability to clear terrestrial obstacles, both with a running start and from standstill. Fig. 10 shows BOLT clearing a 2 cm obstacle, the highest obstacle it can clear with a purely terrestrial gait. In the wings-only configuration the robot is unable to clear the 2 cm obstacle, clearly showing the necessity of the legs. The wings-passive

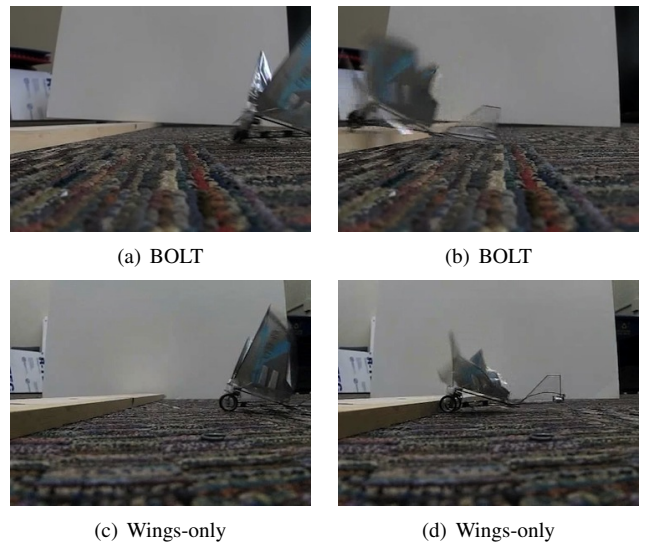


Fig. 10. (a-b) show BOLT running at a 2 cm obstacle and easily clearing the top of it. By contrast, (c-d) show the wings-only robot incapable of getting over the barrier. The wings-passive robot is capable of clearing the barrier, but is not always successful.

robot can clear the obstacle, but does so inconsistently. BOLT has shown two methods of clearing this obstacle, depending on the initial condition when first encountering the obstacle. If the obstacle is encountered at the low point in the stride, the robot will run at the obstacle for a few strides until its legs are able to pull it over the top. During the high point of its stride, the robot simply leaps over the obstacle without stopping. These scenarios are shown in the accompanying video.

V. CONCLUSIONS AND FUTURE WORK

BOLT achieves its goal of being capable of both aerial and terrestrial locomotion, and transitioning between the two in an indoor environment. During dynamic running, BOLT uses a unique method for maintaining passively stable bipedal locomotion, exploiting the aerodynamic effects of its flapping wings. Because of the aerodynamic forces present on the robot, BOLT does not run using a traditional SLIP gait. Despite this fact, the robot is capable of high speed locomotion, “flying” along the ground using a combination of aerodynamic forces and ground reaction forces to propel itself. The hybrid robot also provides a compromise in efficiency across a range of speeds, when compared to the wings-only and wings-passive robots. The legs and wings hybrid configuration is also particularly adept at crossing low obstacles placed in its path without needing to resort to aerial locomotion.

While not the first hybrid aerial/terrestrial robot, BOLT is currently the smallest. Its ability to transition from terrestrial locomotion to aerial locomotion in a small space enables it to take advantage of both modes of transportation, especially in a confined environment. The key contribution setting BOLT apart is the integration of a smart electronics package capable of measuring the dynamics of a fully capable hybrid plat-

form. BOLT has begun to provide insights into the dynamics of wing assisted locomotion, and allows the interactions between legs and wings to be examined.

Future work on BOLT will further explore the dynamics of running with flapping wings, attempting to determine the proper leg stiffness to achieve a stable gait with high efficiency in a terrestrial mode where SLIP does not apply. Additionally, a transmission capable of selectively driving the legs or wings would further improve the efficiency of the robot. By turning off the wings at low terrestrial speeds, or disengaging the legs when flying, the robot can minimize the power lost to unnecessary appendages. Techniques for steering, both in aerial and terrestrial locomotion modes also bear further investigation.

ACKNOWLEDGMENTS

The authors gratefully thank Stan Baek for his design of the ImageProc 2.2 electronics board, and Stan and Aaron Hoover for their diligent work developing the drivers for the electronics board.

REFERENCES

- [1] P. Birkmeyer, K. Peterson, and R. Fearing, "DASH: A dynamic 16g hexapedal robot," in *IEEE/RSJ International Conference on Intelligent Robots and Systems*, October 2009, pp. 2683–2689.
- [2] A. Hoover, S. Burden, X. Fu, S. Sastry, and R. Fearing, "Bio-inspired design and dynamic maneuverability of a minimally actuated six-legged robot," in *3rd IEEE RAS and EMBS International Conference on Biomedical Robotics and Biomechatronics (BioRob)*, September 2010, pp. 869–876.
- [3] J. M. Morrey, B. Lambrecht, A. D. Horchler, R. E. Ritzmann, and R. D. Quinn, "Highly mobile and robust small quadruped robot," in *IEEE/RSJ International Conference on Intelligent Robots and Systems*, October 2003, pp. 82–87.
- [4] J. G. Cham, S. A. Bailey, J. E. Clark, R. J. Full, and M. R. Cutkosky, "Fast and robust: Hexapedal robots via shape deposition manufacturing," *International Journal of Robotics Research*, vol. 21, no. 10, 2002.
- [5] S. Kim, J. E. Clark, and M. R. Cutkosky, "isprawl: Design and tuning for high-speed autonomous open-loop running," *International Journal of Robotics Research*, vol. 25, no. 9, pp. 903–912, 2006.
- [6] U. Saranli, M. Buehler, and D. E. Koditschek, "Rhex: A simple and highly mobile hexapod robot," *International Journal of Robotics Research*, vol. 20, no. 7, pp. 616 – 631, July 2001.
- [7] N. Neville, M. Buehler, and I. Sharf, "A bipedal running robot with one actuator per leg," in *IEEE International Conference on Robotics and Automation*, May 2006, pp. 848 –853.
- [8] R. Full and M. Tu, "Mechanics of rapid running insects: two-, four-, and six-legged locomotion," *Journal of Experimental Biology*, vol. 156, pp. 215–231, 1991.
- [9] P. Holmes, R. J. Full, D. Koditschek, and J. Guckenheimer, "The dynamics of legged locomotion: Models, analyses, and challenges," *SIAM Review*, vol. 48, no. 2, pp. 207–304, 2006.
- [10] R. Blickhan and R. J. Full, "Similarity in multilegged locomotion: Bouncing like a monopode," *Journal of Comparative Physiology A: Neuroethology, Sensory, Neural, and Behavioral Physiology*, vol. 173, no. 5, pp. 509–517, November 1993.
- [11] D. Lentink, S. Jongerius, and N. Bradshaw, "The scalable design of flapping micro-air vehicles inspired by insect flight," *Flying Insects and Robots*, p. 185, 2009.
- [12] (2011). [Online]. Available: <http://www.ornithopter.org/>
- [13] (2011). [Online]. Available: <http://www.avinc.com/nano>
- [14] R. J. Bachmann, F. J. Boria, R. Vaidyanathan, P. G. Ifju, and R. D. Quinn, "A biologically inspired micro-vehicle capable of aerial and terrestrial locomotion," *Mechanism and Machine Theory*, vol. 44, no. 3, pp. 513 – 526, 2009, special issue on Bio-Inspired Mechanism Engineering.
- [15] F. Boria, R. Bachmann, P. Ifju, R. Quinn, R. Vaidyanathan, C. Perry, and J. Wagener, "A sensor platform capable of aerial and terrestrial locomotion," in *IEEE/RSJ International Conference on Intelligent Robots and Systems*, August 2005, pp. 3959–3964.
- [16] M. Kovac, J. Zufferey, and D. Floreano, "Towards a self-deploying and gliding robot," *Flying Insects and Robots*, 2009.
- [17] M. Kovac, J. Germann, C. Hrzeler, R. Siegwart, and D. Floreano, "A perching mechanism for micro aerial vehicles," *Journal of Micro-Nano Mechatronics*, vol. 5, pp. 77–91, 2009.
- [18] A. Lussier Desbiens, A. Asbeck, and M. Cutkosky, "Landing, perching and taking off from vertical surfaces," *The International Journal of Robotics Research*, vol. 30, no. 3, p. 355, 2011.
- [19] D. Lachat, A. Crespi, and A. Ijspeert, "Boxybot: a swimming and crawling fish robot controlled by a central pattern generator," in *The First IEEE/RAS-EMBS International Conference on Biomedical Robotics and Biomechatronics (BioRob)*, February 2006, pp. 643–648.
- [20] C. Georgiades, A. German, A. Hogue, H. Liu, C. Prahacs, A. Ripsman, R. Sim, L. Torres, P. Zhang, M. Buehler *et al.*, "AQUA: an aquatic walking robot," in *IEEE/RSJ International Conference on Intelligent Robots and Systems*, vol. 4, September 2004, pp. 3525–3531.
- [21] M. Bundle and K. Dial, "Mechanics of wing-assisted incline running (WAIR)," *Journal of Experimental Biology*, vol. 206, no. 24, pp. 4553–4564, 2003.
- [22] R. Wood, S. Avadhanula, R. Sahai, E. Steltz, and R. Fearing, "Micro-robot design using fiber reinforced composites," *Journal of Mechanical Design*, vol. 130, p. 052304, 2008.
- [23] S. Baek, F. G. Bermudez, and R. Fearing, "Flight control for target seeking by 13 gram ornithopter," in *IEEE International Conference on Intelligent Robots and Systems (IROS)*, September 2011.